Astron. Astrophys. 335, 995–1002 (1998)

ASTRONOMY
AND
ASTROPHYSICS

# Line profile variability in the spectrum of the O(f) supergiant HD 192639⋆

**G. Rauw and J.-M. Vreux**

Institut d'Astrophysique et de Géophysique, Université de Liège, 5, Avenue de Cointe, B-4000 Liège, Belgium

Received 16 January 1998 / Accepted 16 March 1998

**Abstract.** We report the results of a medium-resolution spectroscopic investigation of the O(f) supergiant HD 192639. Particular attention is paid to the He II $\lambda$ 4686 line. This line displays strong profile variability on time scales of a few days, changing from a P-Cygni profile with a double-peaked emission component to a pure blue-shifted emission line. It appears that the variability of most of the absorption lines present in our spectra is correlated to the deformation of the He II $\lambda$ 4686 line and arises probably from a large scale structure in the low-velocity part of the stellar wind rather than from a photospheric phenomenon. We find that the time scale of the variability could be consistent with the estimated rotational period of HD 192639.

**Key words:** line: profiles – stars: early-type – stars: mass loss – stars: individual: HD 192639 – stars: variables: other – supergiants

## 1. Introduction

Spectroscopic variability in the optical and ultraviolet wavebands is a widely observed characteristic of early-type stars. However, in most cases, the underlying mechanisms are still rather ill-defined. Only an extensive spectroscopic investigation allows to derive constraints on the time scales and the properties of these variations. The typical time scales range from a few hours to several days (e.g. Fullerton et al. 1996, Kaper et al. 1996, 1997). One of the most controversial issues is the connection between the variability at the photospheric level and in the stellar wind. In some stars, the line profile variability of photospheric absorption lines is attributed to pulsations (e.g. Kambe et al. 1997), whereas Kaper et al. (1997) suggest that a stellar magnetic field may be an essential ingredient for controlling wind variability.

In the present paper, we focus our attention on HD 192639, a rather poorly studied member of the Cyg OB1 association. On the basis of eye inspection of photographic spectra, Walborn (1972) assigned a spectral type O7 Ib (f) to this star; the tag (f) in this classification scheme indicates that the N III $\lambda\lambda$ 4634-41 lines are clearly seen in emission whereas the He II $\lambda$ 4686 line is seen neither clearly in emission nor in absorption. Using quantitative criteria, namely the ratio of the equivalent widths of selected lines, Conti & Alschuler (1971) assigned a spectral type O7.5 III f to HD 192639. More recently, using the same quantitative criterion on her spectra, Underhill (1995a) derived an O8 spectral type instead of O7 or O7.5. On the basis of the Stark broadening of the He II lines, Underhill (1995b) further assigned a supergiant luminosity class to HD 192639, leading to a O8 I f classification.

In the HR-diagram of the Cyg OB1 association HD 192639 lies at a position typical for a blue straggler, i.e. beyond the turnoff point of the association and in the vicinity of the continuation of the ZAMS (Mathys 1987). The spectrum of HD 192639 shows some indication for the presence of CNO processed material at the surface of the star. In fact, Schild & Berthet (1986) found that the C/N abundance ratio is smaller in HD 192639 than in HD 193514, another member of the Cyg OB1 association with a similar spectral type. Herrero et al. (1992) also derived a slightly enhanced helium abundance in the spectrum of HD 192639.

Variability of the emission lines in the spectrum of HD 192639 has already been reported on various occasions (Mannino & Humblet 1955, Underhill 1995a). Underhill (1995a) noticed line profile variability over a few days in the H$\alpha$ and He II $\lambda$ 4686 emission lines. Fullerton et al. (1996) discovered the existence of line profile variability in the C IV $\lambda\lambda$ 5801, 5812 absorption lines and in the He I $\lambda$ 5876 P-Cygni profile over an interval of about seven days. Finally, in the near infrared, Andrillat & Vreux (1979) reported the variability of the He I $\lambda$ 10830 emission line, also on a time scale of a few days.

## 2. Observations and data reduction

A first snapshot spectrum of HD 192639, covering the wavelength range 4530 - 4720 Å, was taken in July 1995 (JD 2449913.54) with the Carelec spectrograph attached to the 1.93 m telescope of the Observatoire de Haute-Provence. The spectrum was obtained in the second order with a 1200 lines/mm grating blazed at 7500 Å, providing a reciprocal dispersion of

*Send offprint requests to*: G. Rauw

⋆ Based on observations collected at the Observatoire de Haute Provence, France.

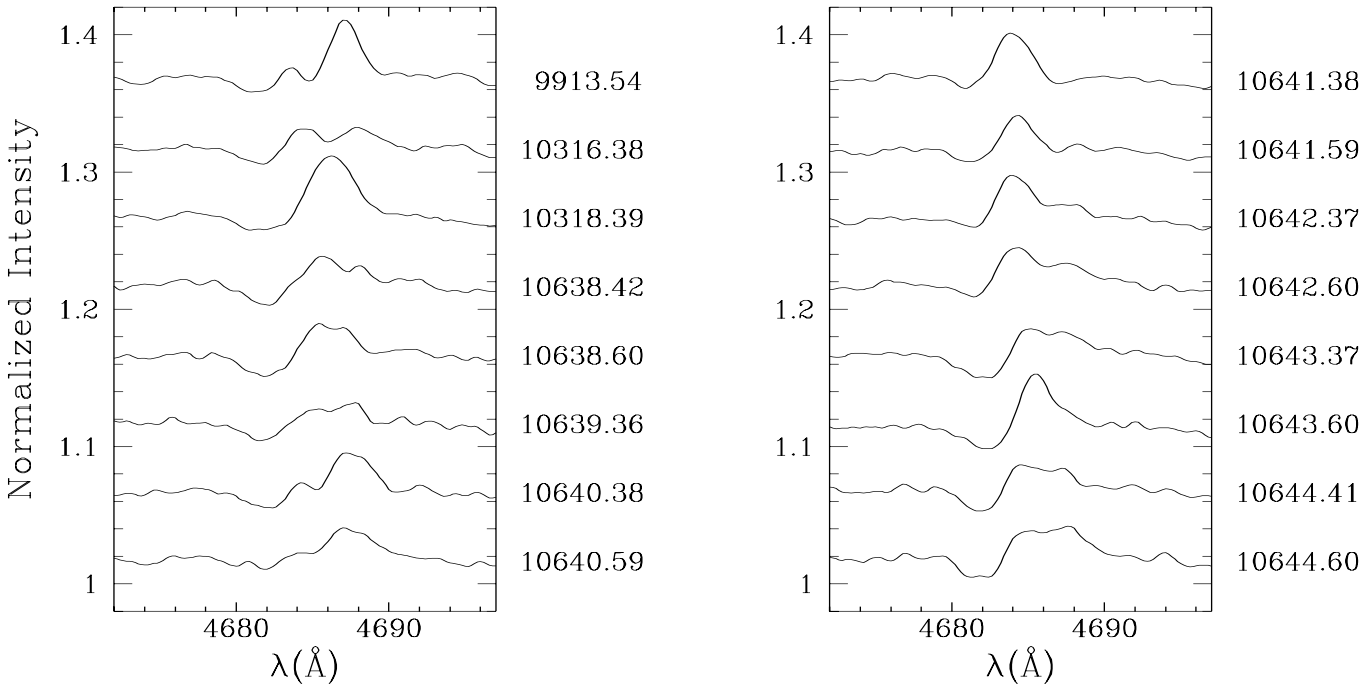


**Fig. 1.** Examples of the variability of the He II $\lambda$ 4686 line profile in the normalized spectrum of HD 192639 as a function of time. The different spectra are shifted vertically by 0.05 units. The epochs of the observation (JD-2440000) are indicated on the right side of each spectrum.

17 Å/mm. The detector was a Tektronix TK512 CCD with a pixel size of 27$\mu$m. The spectral resolution as derived from the FWHM of the lines in the NeAr calibration exposures is $\sim$ 1.0 Å.

A more extensive set of spectroscopic observations of HD 192639 was secured during two observing campaigns in August 1996 and July 1997 with the Aurélie spectrograph (Gillet et al. 1994) fed by the 1.52 m telescope of the Observatoire de Haute-Provence. The data were obtained with a 300 lines/mm grating blazed at 6000 Å providing a reciprocal dispersion of 33 Å/mm over a wavelength range from 4100 to 4950 Å. The detector was a Thomson TH7832 linear array with a pixel size of 13 $\mu$m. Two spectra were taken in 1996 (JD 2450316.38, 2450318.39), while a total of 25 spectra of HD 192639 were obtained over seven nights in 1997 (JD 2450638.42 – 2450644.60). The mean exposure time was 30 minutes and the mean S/N ratio in the continuum of the raw spectra is $\sim$ 200. Comparison exposures of a ThAr lamp were taken for each stellar spectrum. The spectral resolution as derived from the FWHM of the calibration lines is $\sim$ 1.2 Å.

All the data were reduced in the standard way using the MIDAS software developed at ESO.

The spectra were normalized using properly chosen continuum windows. As for many Of stars, there is a broad emission bump between $\lambda$ 4600 and $\lambda$ 4700 in the spectrum of HD 192639. The normalized line profiles shown in Figs. 1 and 3 therefore include a weak contribution from this underlying emission feature.

## 3. Results

### *3.1. The He* II *$\lambda$ 4686 line*

The profile variability of this line is illustrated in Fig. 1. We notice different kinds of P-Cygni profiles. On several occasions, we can see a double peaked emission with varying intensities of the components. Sometimes both have the same intensity (e.g. JD 2450316.38, 2450638.60,...). On other spectra either the red component (e.g. JD 2449913.54, 2450640.38,...), or the blue component (e.g. JD 2450642.37) is the dominant one. Normal P-Cygni profiles are also observed (e.g. JD 2450318.39, 2450643.60). On the spectra taken during the night JD 2450641, we observe a blue-shifted emission line with weak absorption components on both sides. An even more extreme blueward excursion of the emission component was observed by Underhill (1995a) on 1991 September 24. At that time, the profile consisted of a weak broad emission feature with a very weak absorption component on the longward edge.

We have measured the equivalent widths of the absorption and the emission components of the line. The EWs of the entire profile display some variability, during each night and from night to night. In July 1997, the maximum total EW is observed around JD 2450642.5.

Fig. 2a displays the variability of the equivalent width of the absorption component. This measurement includes the very weak red absorption component that appears when the emission line reaches its most negative radial velocity. One notices that the intensity of the absorption component progressively decreases over five nights before it jumps back to its initial high value (JD 2450643).

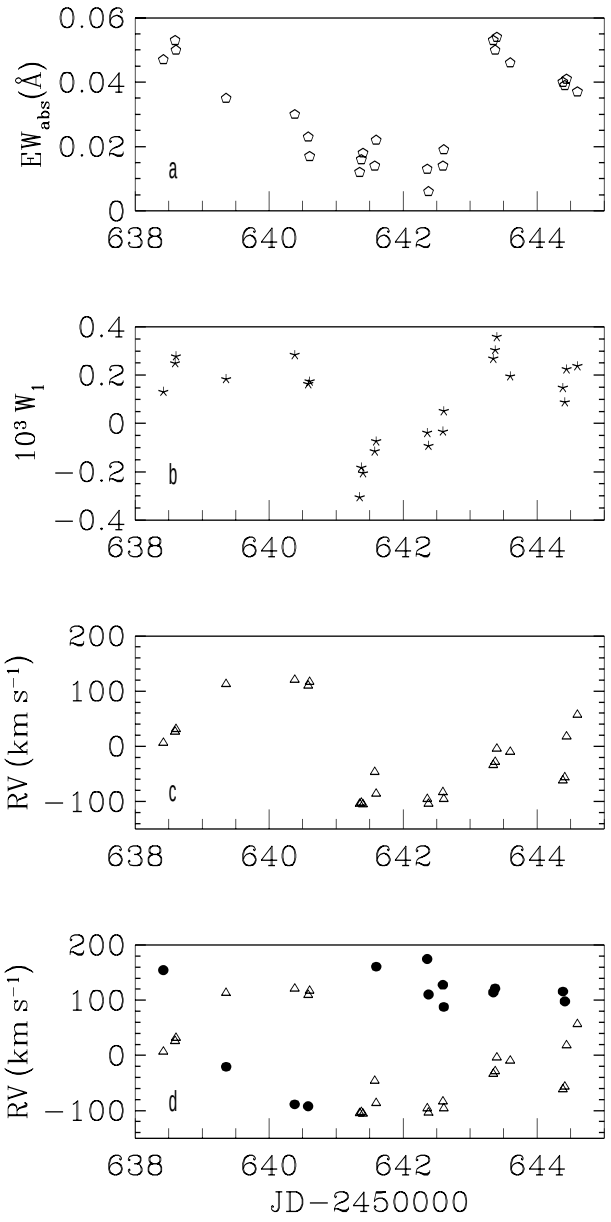


**Fig. 2. a** Equivalent width of the absorption component of the He II $\lambda$ 4686 line in the spectrum of HD 192639 as observed during our campaign in July 1997. **b** First order moment of the profile of the He II $\lambda$ 4686 line integrated between $\lambda$ 4675.8 and $\lambda$ 4695.8 (see text). **c** Radial velocity of the strongest peak of the emission component of He II $\lambda$ 4686. **d** Same as **c** but this time we have also plotted the RVs of the second highest peak in the emission component (filled circles).

An easy means to quantify the line profile variability is through the so-called moments of the line. Let us recall that the $n$th order moment of a line is defined by (e.g. Castor et al. 1981):

$$W_n = \left(\frac{c}{\lambda_0\, v_\infty}\right)^{n+1} \int_{\rm line} \left(\frac{F_\lambda}{F_c} - 1\right) (\lambda - \lambda_0)^n \, d\lambda \qquad (1)$$

where $F_\lambda$ is the flux of the line and $F_c$ is the corresponding continuum flux. $\lambda_0$ and $v_\infty$ designate the rest wavelength of the line and the terminal velocity of the wind respectively. In our present analysis, we focus on the first order moment, since it provides a direct measurement of the asymmetry of the line. We adopt a terminal velocity of 2180 km s$^{-1}$ (Prinja et al. 1990) and we integrate the profile between $\lambda$ 4675.8 and $\lambda$ 4695.8.

The variations of $W_1$ as a function of time are shown in Fig. 2b. $W_1$ shows no systematic trend except during the blueward excursion of the dominant emission peak when the first order moment becomes negative.

The radial velocities of the dominant peak of the emission component, determined by fitting a gaussian, are displayed in Fig. 2c. We observe variations over a range of some 200 km s$^{-1}$. Finally, for those spectra on which the emission component appears double-peaked, the radial velocities of both peaks are shown in Fig. 2d. The latter figure indicates that the RV variations of the strongest peak shown in Fig. 2c seemingly result from the alternating intensities of the two peaks.

### *3.2. Other emission lines*

The normalized spectrum of HD 192639 between $\lambda$ 4625 and $\lambda$ 4660 is illustrated as a function of time in Fig. 3. The relatively intense N III $\lambda\lambda$ 4634-41 emission lines do not display the same behaviour as the He II $\lambda$ 4686 line. In particular, the radial velocities of the N III emission peaks remain nearly constant (see Table 1 below). We notice some intensity variations, that are only slightly correlated to the variations of He II $\lambda$ 4686 (see Fig. 5) and present a much lower relative amplitude than for the latter line.

The formation of the N III $\lambda\lambda$ 4634-41 ($3p\ ^2\mathrm{P}^0 - 3d\ ^2\mathrm{D}$) lines in the atmospheres of O stars has been discussed by Mihalas & Hummer (1973). These authors have shown that in the photosphere of O((f)) and O(f) stars, the $3d\ ^2\mathrm{D}$ level of the $\mathrm{N}^{2+}$ ion is overpopulated as a result of dielectronic recombination, leading to photospheric emission of the $\lambda\lambda$ 4634-41 lines. In the case of HD 192639, the lower amplitude of variation and the different behaviour of the N III lines compared to the He II $\lambda$ 4686 wind feature probably confirm that the former emission lines arise mainly in the photosphere of the star rather than in the stellar wind.

In order to measure the line profile variability in a quantitative way, we have computed the time variance spectrum (TVS, Fullerton et al. 1996) of our Aurélie observations. For the most variable lines in the spectrum of HD 192639, Table 1 provides the value of the highest peak of $(TVS)^{1/2}$ over the entire line profile, the velocity interval $\Delta\, v$ over which the detected variations are significant at the 99% confidence level, as well as the mean amplitude of the deviation $(TVS)^{1/2}$ evaluated over $\Delta\, v$. For the N III $\lambda\lambda$ 4634-4641 emission lines, the severe blending of the TVS features of these lines and the proximity of the variable C III $\lambda\lambda$ 4647-50 absorption lines prevent a reliable evaluation of the mean amplitude. Nevertheless, the TVS parameters given in Table 1 confirm that the N III $\lambda\lambda$ 4634-4641 blend displays a lower variability than e.g. the He II $\lambda$ 4686 line.

Brucato (1971) claimed to detect irregular variations in the equivalent width of the N III emission lines on a time scale of

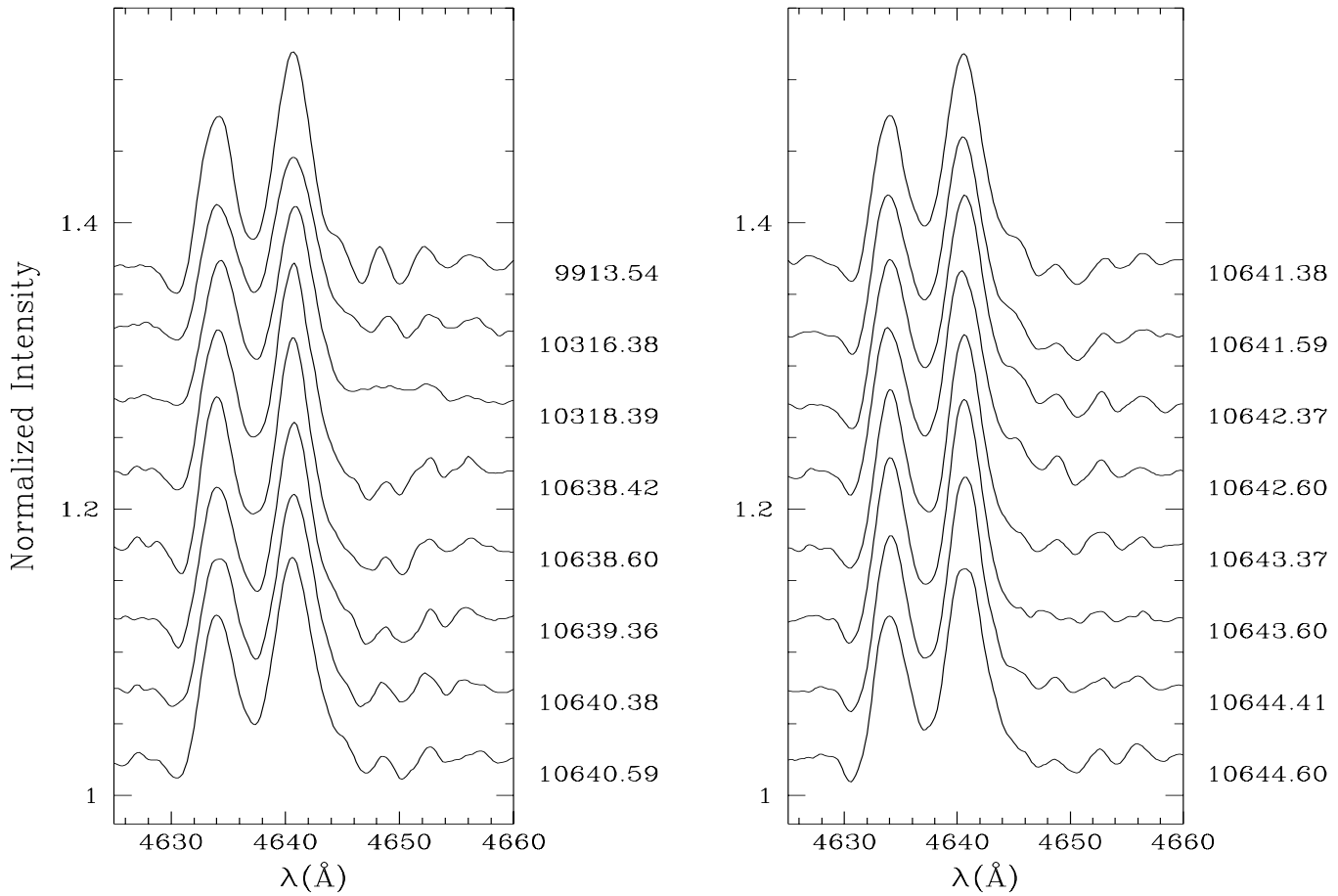


**Fig. 3.** Same as Fig. 1, but for the blend around the N III $\lambda\lambda$ 4634-41 lines in the spectrum of HD 192639. The absorption line shortward of the N III emissions is due to Si IV $\lambda$ 4631. One notices also the important variability of the C III $\lambda\lambda$ 4647, 4650 absorptions (see text).

about 20 minutes. Even if the sampling of our time series is not well suited to detect such rapid fluctuations, it appears that the reliability of Brucato's discovery is rather difficult to assess. In fact, Brucato (1971) noticed these rapid variations only during one night, whereas he found only marginal variability during the other nights. Moreover, these results were derived from photographic plates and the author does not provide error estimates for his measurements.

Concerning the two unidentified emission lines at $\lambda$ 4486 and $\lambda$ 4504, we detect no significant variability and no correlation with the variability of the H$\beta$ line (Fig. 5). We conclude therefore that these lines are probably not produced in the stellar wind, but may arise in the same physical region as the bulk of the N III emission.

### *3.3. The absorption lines*

All the absorption lines in the observed spectral domain display variations to some extent. Part of the intensity variability may result from uncertainties in the normalization of the spectra. We will therefore focus our attention on the strongest lines that show the most stringent variations, as indicated by the TVS analysis (Table 1), and which are the least sensitive to the uncertainties of the normalization.

Fig. 4 displays the variability of the H$\beta$ absorption line in the spectrum of HD 192639. During the observing run in July 1997, the equivalent width of this line varies over a range of $\sim$ 7% (1$\sigma$) around the mean value. Larger deviations from the mean equivalent width are observed in August 1996, when the line appears some 18 - 26% weaker than on the average.

Besides the variations of its intensity, the H$\beta$ line displays also important profile variability (Fig. 4). The core of the line changes from a symmetric nearly gaussian shape to a rather sharp asymmetric minimum, that appears either red-shifted or blue-shifted. Occasionally, we also observe a flat minimum.

We have constructed a dynamical spectrum by assembling quotient spectra obtained after division of the individual data by the mean spectrum. A close inspection of this dynamical spectrum reveals a tight resemblance between the deformation pattern of the H$\beta$, H$\gamma$, He I $\lambda$ 4471 and He II $\lambda$ 4686 lines, in the sense that the stronger is the He II $\lambda$ 4686 emission component, the weaker are the absorption lines.

To quantify this impression, we have used the local pattern cross-correlation technique discussed by Vreux et al. (1992) and by Gosset et al. (1994). Some results obtained using the H$\beta$ line

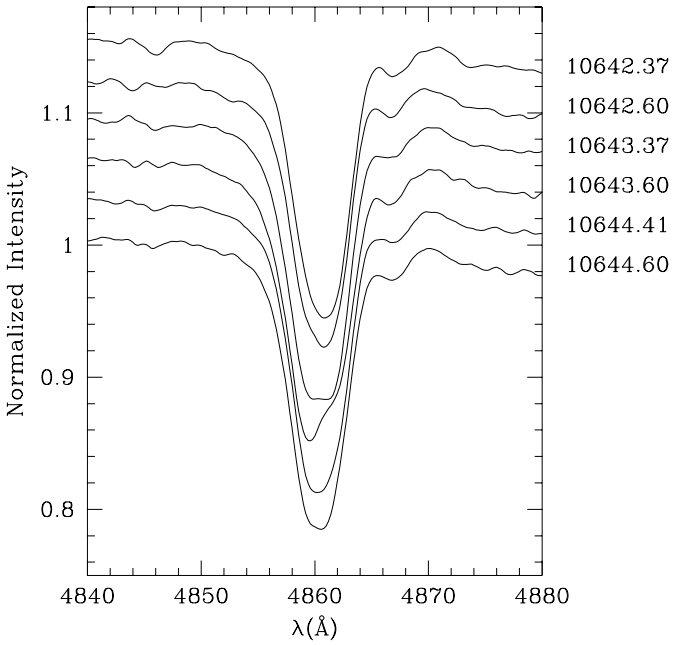


**Fig. 4.** Illustration of the variability of the shape and strength of the H$\beta$ line as observed during the last three nights of the July 1997 observing campaign. For each night, we show the mean spectrum of the first and second half of the night. The different spectra are shifted vertically by 0.03 units.

as a reference are shown in Fig. 5. This figure underlines the strong correlation between the mean deformation pattern of the different lines in the spectrum of HD 192639.

In Fig. 3 we notice the strong changes in the visibility of the C III $\lambda\lambda$ 4647-50 absorption lines. On JD 2450318.39 and JD 2450643.60, these lines have nearly disappeared, whereas they present their maximum intensity on JD 2449913.54 and JD 2450640.59. The cross-correlation method indicates that the deformation pattern of these lines is correlated to the one of the H$\beta$ line (Fig. 5).

The correlations between the profile variations of the absorption lines and those of the He II $\lambda$ 4686 emission suggest that the bulk of the variability of the absorption line profiles in the spectrum of HD 192639 is produced by a variable stellar wind emission rather than by a genuine photospheric phenomenon.

Our results are in good agreement with the conclusions of previous studies. Underhill (1995a) noticed that the leading members of the He I series are displaced shortwards by some 11 km s$^{-1}$ indicating that the cores of the strong He I lines are formed in the wind. The same holds true for the Balmer lines H$\beta$ and H$\gamma$. Herrero et al. (1992) also noticed a strong dilution effect of the He I $\lambda$ 4471, H$\gamma$ and H$\beta$ lines due to a stellar wind. In the same context, Fullerton (1990) noticed the strong resemblance between the variations of the C IV $\lambda\lambda$ 5801, 5812 absorption lines and those of the absorption trough of the He I $\lambda$ 5876 P-Cygni profile. From these results, Fullerton et al. (1996) conclude that the variability of the C IV doublet in the spectrum of HD 192639 is probably not consistent with a purely photospheric origin.

We have measured the equivalent widths of several strong, unblended lines in the spectrum of HD 192639. The average values and the standard deviations are listed in Table 1. Of particular interest are the classification lines He I $\lambda$ 4471 and He II $\lambda$ 4542. During the 1997 observing campaign, the standard deviations of the EWs of these lines amount respectively to 7% and 5% of their intensity (Table 1). As for most of the absorption lines, the EWs of the He I $\lambda$ 4471 and He II $\lambda$ 4542 lines are the weakest in August 1996, when the intensities deviate by some 14% from their mean values. Considering our whole dataset, the O-star classification criterion $\log_{10} W' = \log_{10}\left(\frac{EW(4471)}{EW(4542)}\right)$ (Conti 1973) varies between 0.066 and 0.173, i.e. around the border line between spectral types O7.5 and O8, with an average value of $0.115 \pm 0.029(1\sigma)$ corresponding to spectral type O8. However, one has to bear in mind that at least the He I $\lambda$ 4471 line and possibly also the He II $\lambda$ 4542 line are partially filled in by emission from the stellar wind and their EWs therefore do not depend on the temperature of the photosphere alone.

Since the cores of most of the absorption lines are formed in the wind, one has also to be careful when deriving the chemical composition of the star using a plane parallel model atmosphere. As a matter of fact, the optical depth of the wind for different transitions not only depends on the abundances of the corresponding ions, but also on the physical conditions in the wind.

In order to search for long-term changes, we have compared the equivalent widths listed in Table 1 to the average values reported in the literature (Oke 1954, Mannino & Humblet 1955, Underhill 1995b). We find a very good agreement between our values and the EWs of Underhill (1995b). On the other hand, the older determinations yield systematically larger EWs than our data, although the various datasets usually agree within the limits set by the estimated errors and the observed range of variability. The most outstanding differences concern the He I $\lambda\lambda$ 4471, 4713 and He II $\lambda$ 4542 lines that appeared some 15 - 40% stronger during the older observations (Oke 1954, Mannino & Humblet 1955). Whether or not these differences reflect a genuine long-term change is however not clear since a reliable estimate of the error bars on the oldest photographic EW determinations is lacking.

### *3.4. Radial velocities*

Conti et al. (1977) found that the radial velocity of HD 192639 was probably variable over a small range. Later on, Underhill (1995a) suggested that HD 192639 could be a single-lined spectroscopic binary with an orbital period of a few days.

Binarity could be a possible interpretation of the observed deformations of the He II $\lambda$ 4686 line. Strong line profile variability in this line is indeed expected to occur as a consequence of colliding winds in early-type binary systems (Rauw 1997). However, the small range of radial velocity variations would probably indicate a low orbital inclination and the expected line profile variability drastically decreases for lower inclinations. Therefore, it seems unlikely that wind interactions in a binary

**Table 1.** Measured characteristics of the most prominent lines in the blue-violet spectrum of HD 192639. The second column gives the time-averaged radial velocities, whereas the fourth column lists the equivalent widths of the strongest unblended absorption lines. The last three columns provide the results of the TVS analysis for those lines that display significant variability (see text). The amplitude of $(TVS)^{1/2}$ is expressed as a percentage of the normalized continuum flux. The velocity intervals labelled with a colon are uncertain due to the severe blending of the N III emission lines.

| Line | Mean RV (km s$^{-1}$) | $\sigma$(RV) (km s$^{-1}$) | Mean EW (Å) | $\sigma$(EW) (Å) | max $(TVS)^{1/2}$ [%] | $\Delta\, v$ km s$^{-1}$ | Mean $(TVS)^{1/2}$ [%] |
|---|---|---|---|---|---|---|---|
| absorption lines | | | | | | | |
| He II $\lambda$ 4200 | $-3.8$ | 9.1 | 0.435 | 0.036 | 0.95 | $-270$ , $+260$ | 0.69 |
| H$\gamma$ | $-33.8$ | 7.0 | 1.457 | 0.086 | 1.84 | $-385$ , $+390$ | 1.04 |
| He I $\lambda$ 4388 | $-8.1$ | 7.1 | | | | | |
| He I $\lambda$ 4471 | $-15.8$ | 6.2 | 0.621 | 0.044 | 1.21 | $-460$ , $+330$ | 0.62 |
| N III $\lambda$ 4511 | 7.1 | 7.6 | | | | | |
| N III $\lambda$ 4515 | $-3.4$ | 5.9 | | | | | |
| He II $\lambda$ 4542 | 0.9 | 3.3 | 0.476 | 0.025 | 0.82 | $-315$ , $+215$ | 0.49 |
| He I $\lambda$ 4713 | $-5.1$ | 4.1 | 0.187 | 0.013 | | | |
| H$\beta$ | $-41.2$ | 11.3 | 1.355 | 0.127 | 2.56 | $-430$ , $+600$ | 1.14 |
| He I $\lambda$ 4922 | $-6.9$ | 5.9 | 0.216 | 0.017 | | | |
| emission lines | | | | | | | |
| N III $\lambda$ 4634 | $-0.2$ | 4.6 | | | 0.61 | $-290$ , $+110$ : | $\leq$ 0.45 : |
| N III $\lambda$ 4641 | $-13.2$ | 5.1 | | | 0.78 | $-235$ , $+115$ : | $\leq$ 0.57 : |
| He II $\lambda$ 4686 | | | | | 1.37 | $-440$ , $+265$ | 0.69 |

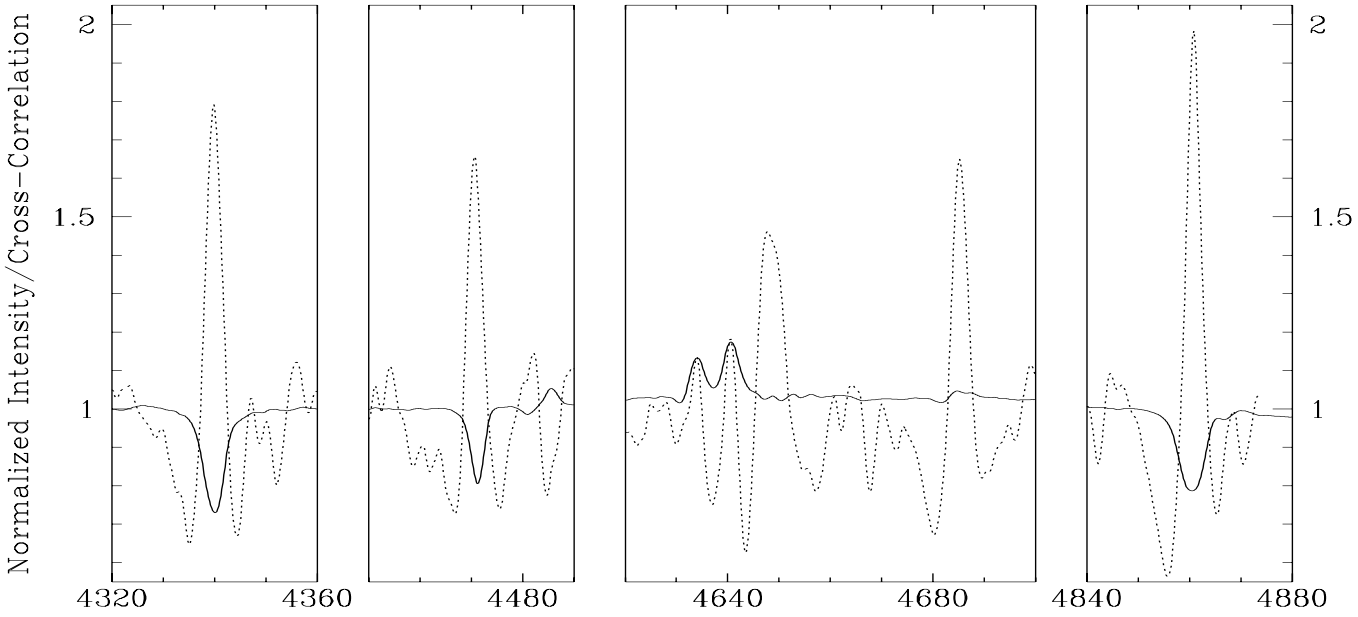


**Fig. 5.** Mean result of the local pattern cross-correlation on the dynamical quotient spectra using the deformation pattern of the H$\beta$ line as a reference (see Sect. 3.3 for details). The cross-correlation has been shifted up by one unit and is superimposed on the mean spectrum of HD 192639 (continuous line). The broad peak around $\lambda$ 4650 in the cross-correlation spectrum is due to the C III $\lambda\lambda$ 4647-50 lines. The width of the reference H$\beta$ pattern (12Å) does not allow to separate the individual cross-correlation peaks of the two C III lines.

system could account for the deformations of the He II $\lambda$ 4686 line observed in the spectrum of HD 192639.

We have measured the radial velocities of the most prominent absorption lines in our spectra. The central wavelengths of the absorption lines are determined by fitting Gaussian profiles and the radial velocities are computed with respect to the effective wavelengths tabulated by Conti et al. (1977). The results are given in Table 1 and the mean radial velocity of ten absorption lines is shown as a function of time in Fig. 6. This mean radial velocity has an average value and a standard deviation of respectively $-8.1$ km s$^{-1}$ and 5.0 km s$^{-1}$. The range of radial velocity variability of the different lines, quoted in Table 1, is in good agreement with the results of Fullerton (1990). Fig. 6 shows that the radial velocity of the absorption lines is slightly more positive during two nights (i.e. JD 2450641-642) than on the average. This more positive velocity occurs simul-

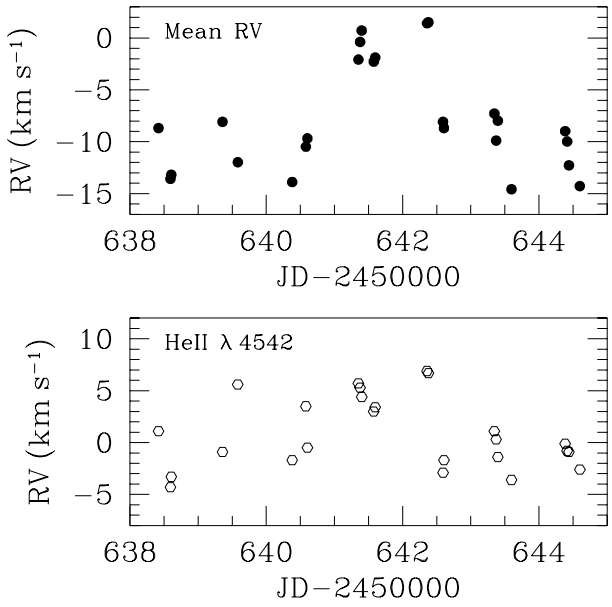


**Fig. 6.** Upper panel: variations of the mean radial velocity of ten absorption lines in the blue-violet spectrum of HD 192639 during the observing run in July 1997. Lower panel: same as above, but for the He II $\lambda$ 4542 line only.

taneously with the minimum of the first order moment of the He II $\lambda$ 4686 line, i.e. when the emission component of the latter line reaches its maximum blueward excursion. However, it seems rather unlikely that the effect seen in Fig. 6 reflects a true velocity variation in a real binary system. In fact, in most of the absorption lines, at least part of the radial velocity variations result from the line profile variability. As discussed above, this variability is probably due to a changing stellar wind emission. On the other hand, the lower panel of Fig. 6 illustrates the radial velocity of the He II $\lambda$ 4542 line as a function of time. This line presents a slightly lower line profile variability and is probably less affected by emission from the stellar wind (Herrero et al. 1992) than some of the other lines used to compute the mean velocity. One can see on this figure that the amplitude of velocity variation is also smaller than for the mean of the RVs.

We conclude therefore that the present analysis does not provide any clear indication in favour of a binary nature of HD 192639.

## 4. Discussion

The variability of early-type stellar winds is usually attributed to inhomogeneities or large-scale structures evolving on time scales of several hours to a few days. Large-scale structures in the wind may be connected to photospheric variability through a modulation of the stellar wind by the combined effect of stellar rotation and a moderate magnetic field. An alternative explanation for a photospheric connection could be the instability inherent to radiatively driven stellar winds in the case of a photosphere undergoing non radial pulsations.

Kaper et al. (1997) suggest that the variability in their sample of bright O stars is related to so-called Corotating Interacting Regions. Such corotating stream structures are expected as a result of azimuthal variations in the properties of the outflow as would arise near bright or dark spots on the stellar surface (Cranmer & Owocki 1996). A large-scale wind structure could also result from a strong magnetic field that would confine the wind towards the magnetic equator (Babel & Montmerle 1997). If the magnetic axis is tilted with respect to the rotational axis, the line emitting region near the magnetic equator will be seen under varying inclinations, resulting in periodic line profile variability. Such a configuration is suggested by Stahl et al. (1996) to explain the strictly periodic variability found in the case of HD 37022 (O7 V).

Our observations reveal strong line profile and intensity variations in the spectrum of the O8 I(f) star HD 192639. The changes seen in the absorption lines appear to be correlated to the variability of the He II $\lambda$ 4686 line, suggesting that the phenomenon probably arises in the stellar wind.

The double-peaked shape of the He II $\lambda$ 4686 emission component as well as its variability indicate that the wind of HD 192639 is not spherically symmetric. The variability in the wind of HD 192639 affects the entire He II $\lambda$ 4686 profile and is therefore most probably related to large-scale structures in the low velocity part of the wind rather than to small-scale inhomogeneities.

The characteristic timescales are a key issue for the study of variability in early-type stars. The present data are clearly not sufficient to perform a detailed time series analysis and to find out if the phenomenon observed in the spectrum of HD 192639 is periodic or not. Nevertheless, some of the He II $\lambda$ 4686 profiles we have observed were already seen during earlier snapshot observations by other observers (Underhill 1995a, Herrero et al. 1992), suggesting that the phenomenon is stable over several years. Furthermore, the properties of the He II $\lambda$ 4686 line during the 1997 observing campaign (Fig. 2) suggest that the recurrence time scale could be of the order of 4 - 6 days, although we cannot exclude a somewhat longer time scale. A crude Fourier analysis of the characteristics of the He II $\lambda$ 4686 line over our entire dataset (i.e. including the 1995 and 1996 snapshot observations) yields a recurrence time of $\sim 5$ days. However, since this time scale is comparable with the total time spanned by our 1997 dataset, the meaning of the Fourier analysis is rather difficult to assess. We find no trace of the 2 day recurrence marginally present in the 1986 observations of the C IV $\lambda\lambda$ 5801, 5812 doublet by Fullerton (1990). On the other hand, during the same limited observing run (6 nights), Fullerton (1990) derived a time scale of $4.15 \pm 0.37$ days for the variations of the He I $\lambda$ 5876 line, a value which is more compatible with our results.

Herrero et al. (1992) derive a radius of $19.5\,R_\odot$ for HD 192639. Estimates of the projected rotational velocity $v \sin i$ range from $103\,\mathrm{km\,s^{-1}}$ (Conti & Ebbets 1977) over $110\,\mathrm{km\,s^{-1}}$ (Penny 1996) to $125\,\mathrm{km\,s^{-1}}$ (Herrero et al. 1992). From the two most extreme estimates of $v \sin i$, we derive an upper limit on the actual rotational period of 7.9 to 9.6 days respectively. Considering the critical break-up velocity and using the stellar parameters derived by Herrero et al. (1992), we can set a lower limit on the rotational period of 3.10 days. The

variability of HD 192639 might therefore well be connected to the stellar rotation.

Additional observations over a longer time span are needed to further investigate the properties of the variability seen in the spectrum of HD 192639 and to find out whether or not the phenomenon can be explained by one of the above mentioned scenarios.

*Acknowledgements.* We are grateful to Drs. E. Gosset and J.-P. Swings for their helpful remarks. We wish to thank the referee, Dr. L. Kaper, for his careful reading of the manuscript and his constructive suggestions. We are greatly indebted to the Fonds National de la Recherche Scientifique (Belgium) for multiple supports. This research is also supported in part by contract ARC 94/99-178 "Action de recherche concertée de la Communauté Française" (Belgium) and by contract P4/05 "Pôle d'Attraction Interuniversitaire" (SSTC-Belgium). Partial support through the PRODEX XMM-OM Project is also gratefully acknowledged. The travels to OHP for the observing runs were supported by the Ministère de l'Enseignement Supérieur et de la Recherche de la Communauté Française. The SIMBAD database has been consulted for the bibliography.

## References

Andrillat Y., Vreux J.-M., 1979, A&A 76, 221
Babel J., Montmerle T., 1997, ApJ 485, L29
Brucato R.J., 1971, MNRAS 153, 435
Castor J.I., Lutz J.H., Seaton M.J., 1981, MNRAS 194, 547
Conti P.S., 1973, ApJ 179, 181
Conti P.S., Alschuler W.R., 1971, ApJ 170, 325
Conti P.S, Ebbets D., 1977, ApJ 213, 438
Conti P.S., Leep E.M., Lorre J.J., 1977, ApJ 214, 759
Cranmer S.R., Owocki S.P., 1996, ApJ 462, 469
Fullerton A.W., 1990, PhD Thesis, University of Toronto
Fullerton A.W., Gies D.R., Bolton C.T., 1996, ApJS 103, 475
Gillet D., Burnage R., Kohler D., et al., 1994, A&AS 108, 181
Gosset E., Vreux J.-M., Andrillat Y., 1994, Ap&SS 221, 181
Herrero A., Kudritzki R.P., Vilchez J.M., et al., 1992, A&A 261, 209
Kambe E., Hirata R., Ando H., et al., 1997, ApJ 481, 406
Kaper L., Henrichs H.F., Nichols J.S., et al., 1996, A&AS 116, 257
Kaper L., Henrichs H.F., Fullerton A.W., et al., 1997, A&A 327, 281
Mannino G., Humblet J., 1955, Ann. Ap. 18, 237
Mathys G., 1987, A&AS 71, 201
Mihalas D., Hummer D.G., 1973, ApJ 179, 827
Oke J.B., 1954, ApJ 120, 22
Penny L.R., 1996, ApJ 463, 737
Prinja R.K., Barlow M.J., Howarth I.D., 1990, ApJ 361, 607
Rauw G., 1997, PhD Thesis, University of Liège
Schild H., Berthet S., 1986, A&A 162, 369
Stahl O., Kaufer A., Rivinius Th., et al., 1996, A&A 312, 539
Underhill A.B., 1995a, ApJS 100, 433
Underhill A.B., 1995b, ApJS 100, 461
Vreux J.-M., Gosset E., Bohannan B., Conti P.S., 1992, A&A 256, 148
Walborn N.R., 1972, AJ 77, 312